Pictorial representation and validation of Clar's aromatic sextet theory using molecular electrostatic potentials†‡

Kunduchi Periya Vijayalakshmi and Cherumuttathu H. Suresh*

Received (in Montpellier, France) 4th March 2010, Accepted 24th May 2010
DOI: 10.1039/c0nj00177e

Topographical features of the molecular electrostatic potential (MESP) of a series of polycyclic aromatic benzenoid hydrocarbons have been analyzed at B3LYP/6-31 + G(d,p) and MP2/6-31 + G(d,p) levels of theory to study the relationship between π-electron distribution and Clar's aromatic sextet theory. For all the molecules, MESP isosurface plots provided an unambiguous visual representation of Clar's aromatic sextet theory. For molecules represented using a single dominant Clar structure, a complete agreement of Clar's theory was observed. For benzenoid structures showing more than one Clar structure, MESP isosurface lobes reflected the merger of possible Clar structures, and even in such cases, the most dominant configuration was clearly obtained in the MESP topography. The MESP at the ring critical point (V_{rcp}) of the π-electron cloud of every ring was found to be a good local measure of aromaticity. A hydrogenation scheme was introduced to calculate the aromatic stabilization energy (E_{aroma}) of the peripheral rings. E_{aroma} and V_{rcp} showed a good linear correlation. Furthermore, a linear correlation of V_{rcp} with the widely used geometric index of aromaticity, HOMA, was obtained. Thus, for a visual representation as well as rationalization of Clar's theory, MESP serves as an important descriptor of the π-regions, and V_{rcp} values give further insight into this theory by quantifying the local aromaticity of each ring in the polycyclic aromatic system. The theoretical results presented herein fully support the ideas of Clar's empirical sextet theory—a theory mainly based on experimental findings of the local reactivity of condensed aromatic systems.

Introduction

Aromaticity is one of the most discussed properties in organic chemistry, whose definition and conceptualization remain controversial. The literature is flooded with theoretical and experimental methods aiming to arrive at a unanimous definition.[1] To begin with, the Hückel ($4n + 2$) rule represented an important step towards the comprehension of aromatic concepts.[2,3] Although Hückel's rule is strictly applicable to single ring systems, many polycyclic aromatic hydrocarbons (PAH) systems also follow it, the famous exceptions being pyrene and coronene. It was Clar who made outstanding contributions to the study of PAH systems through his model of the extra stability of $6n$ π-electron benzenoid systems.[4,5] According to the Clar's rule, the Kekule resonance structure[1] having a maximum number of isolated and localized aromatic π sextets and a minimum number of localized double bonds represents the most aromatic and stable case. For instance, in phenanthrene, the central ring of the molecule behaves like an olefin and the other two rings resemble mostly benzene (*cf.* Fig. 1). The arrow in chrysene given in Fig. 1 indicates the migration of a sextet of π-electrons from one ring to an adjacent ring, which will lead to the formulation of a new Clar structure. Clar structures offer valuable insights into the local reactivities of benzenoid hydrocarbons. Rings with benzenoid sextets are considered to be the most aromatic and kinetically stable. The other rings are less aromatic and are chemically more reactive.

Clar's theory has many experimental confirmations,[5–8] and several theoretical studies have offered a justification[9–12] for it. Randić's extensive review on aromaticity states the ease of Clar's model in understanding and predicting many properties of benzenoid hydrocarbons in a qualitative manner, without complicated calculations.[1] Recently, Portella *et al.* made an assessment of Clar's rule by means of PDI, NICS and HOMA indicators of local aromaticity.[13] Misra *et al.*,[14] in a very recent report, described the quantitative formulation of Clar's concept based on resonance energy, bond length and the local aromaticity criteria of NICS. In general, studies on the quantitative aspects of aromaticity have been focused on structural, magnetic and energetic criteria, and aromaticity indices such as HOMA (Harmonic Oscillator Model for Aromaticity), NICS (Nucleus Independent Chemical Shift), RE (Resonance Energy) and ring current are widely in use.[13–26]

Computational Modeling and Simulation Section, National Institute for Interdisciplinary Science and Technology (CSIR), Trivandum 695 019, India. E-mail: sureshch@gmail.com; Fax: +91 0471-2491712; Tel: +91 0471-2515264

† Electronic supplementary information (ESI) available: Optimized structures and energies of PAH systems at DFT and MP2 levels. See DOI: 10.1039/c0nj00177e

‡ Dedicated to Professor Shridhar R. Gadre on the occasion of his 60th birthday.

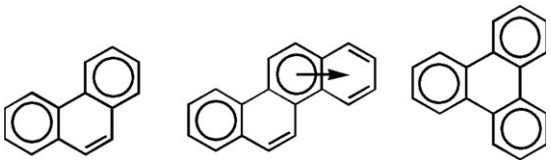

Fig. 1 Clar structures of phenanthrene, chrysene and triphenylene.

Aromaticity is a phenomenon closely related to the extent of electron delocalization in a molecule. Even though electron density is an experimentally accessible quantity,[27] electron delocalization is a very difficult concept to extract directly from the topology of the electron density. However, cleverly designed schemes have recently been developed using electron density topology to study aromaticity.[28,29] The idea of analyzing the topology of charge distribution in real space was first put forward by Bader,[30] and it has been applied to the description of various chemical phenomena. Molecular electrostatic potential (MESP) is a scalar electronic property that shows a close relationship to electron density and charge distribution, and is used widely to understand molecular structure and reactivity.[31–40] MESP contour maps provide useful pictorial information regarding the charge distribution of molecular systems. Previous studies by Suresh and Gadre[36] on polycyclic aromatic hydrocarbons (PAH) showed that the MESP topological properties can give valuable information on Clar's aromatic concepts. Following this earlier work, herein, we study the MESP topographical features of a wide variety of PAH systems (Fig. 2). IUPAC nomenclature is used to name the molecules in Fig. 2.[41] The main focus of the study will be the visualization of Clar's concepts using MESP isosurface features of their π-electron region. Furthermore, attempts will be made to quantify the local aromaticity of arene rings using topographical information.

The MESP is rigorously calculated from the electron density, $\rho(\boldsymbol{r})$, distribution using eqn (1), where Z_A is the charge on nucleus A located at $\boldsymbol{R}_A$.

$$V(r) = \sum_{A}^{N} \frac{Z_A}{|\boldsymbol{r} - \boldsymbol{R}_A|} - \int \frac{\rho(\boldsymbol{r}')d^3\boldsymbol{r}'}{|\boldsymbol{r} - \boldsymbol{r}'|} \qquad (1)$$

Recently, we have reported an MESP-based QSAR study to explain the carcinogenic activity of unsubstituted planar PAHs.[42] Further studies on diol epoxide derivatives of PAHs showed that aromaticity is a key element in determining their carcinogenic potential.[43] We also report the HOMA index of aromaticity,[15] as well as the relative hydrogenation energy of the aromatic rings of selected PAH systems presented in Fig. 2.

Methodology

The geometries of all the compounds have been optimized at the B3LYP/6-31 + G(d,p) DFT level as well as the MP2/6-31 + G(d,p) *ab initio* level using the Gaussian03 suite of programs.[44] The computationally less expensive DFT method is used to calculate the energy of hydrogenation in selected peripheral rings of the PAH systems. For convenience, the rings of all the PAHs are labelled using R_K, R_L, R_M, R_N and R_E notations, where the subscripts K, L, M and N have resemblance to the π-region theory of carcinogenic activity of PAHs[42] and 'E' is used for the empty ring. Thus E, L, K, N and M rings have 0, 1, 2, 3 and 4 consecutive C–H bonds, respectively. For molecules with more than one of the above mentioned rings, numerical subscripts are used to differentiate them, *e.g.* R_{K1}, R_{K2}, *etc*. In the MESP topography, the critical points (CP) are classified into four types, depending on the number of non-zero eigenvalues (*rank*) of the Hessian and

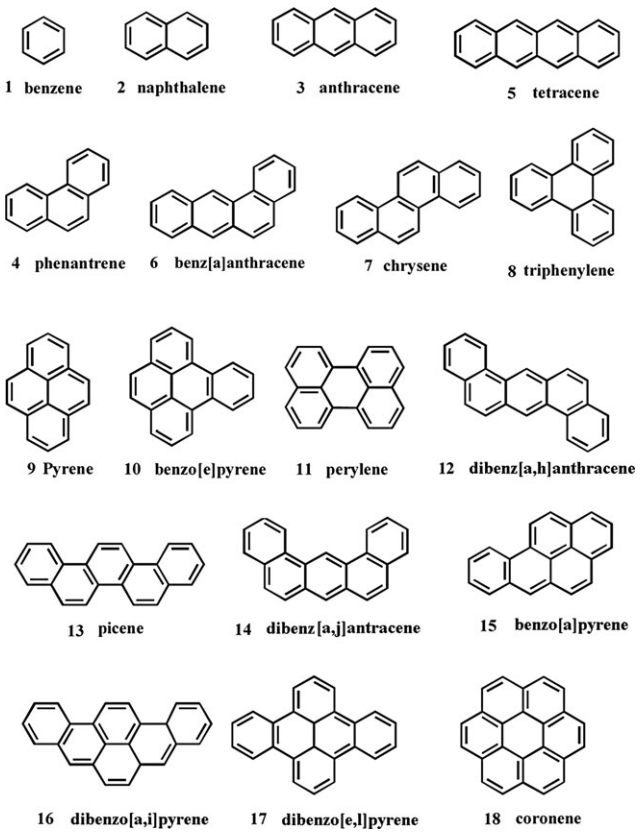

Fig. 2 Benzene and other PAH systems selected for this study. The numbering used to represent these molecules is also given, along with their names.

algebraic sum of their signs (*signature*).[45] A CP is usually represented as an ordered pair of (*rank*, *signature*). Thus, a (3, +3) CP denotes a local minimum with all non-zero eigenvalues, all being positive. Such CPs would appear for lone pair regions and bonds. A bond critical point (bcp) is characterized as a (3, −1) CP, representing a minimum along the direction of a bond and a maximum in two perpendicular directions. A positively valued (3, +1) CP manifests to a ring, and positive or negatively valued saddles may also appear connecting all other CPs. Herein, the MESP ring CP of the π-region (designated as V_{rcp}) is calculated at both DFT and MP2 levels. All the V_{rcp} points were calculated using the UNIVIS program.[46,47] The V_{rcp} of the π-region is found to be a (3, −1) saddle. At the DFT level, the M and N π-regions did not show the clear formation of V_{rcp} CPs as these regions were very shallow and the threshold of the convergence of the gradient was difficult to achieve. Therefore, at this level, numerical evaluation of V_{rcp} was made for the M and N π-regions by computing the MESP on a fine grid using Gaussian03.

Results and discussion

MESP isosurface features and ring CP at π-region of aromatic rings

Herein, a number of condensed PAHs are examined with an aim of identifying the aromatic properties of benzenoid

molecules in relation to their MESP. To begin with, the MESP contour maps are generated at the B3LYP level, as well as the MP2 level, of theory using the basis set 6-31 + G(d,p). The mode of distribution of π-electrons in a given hexagon in a PAH is well represented in the MESP map depicted in Fig. 3. The appearance of the DFT and MP2 level isosurface maps are nearly identical, except for the values they represent. On comparing the distribution of MESP lobes at the isosurface value around 11 kcal mol^{-1} at the DFT level and 14 kcal mol^{-1} at the MP2 level with the most probable Clar structures of these PAHs (Fig. 3), a clear-cut illustration of Clar's aromatic sextet theory is exposed. Molecules with Clar's sextets are characterized by the presence of MESP lobes contained within the boundary of the corresponding hexagon. Hence, the MESP features of benzenoids are assumed to carry a substantial amount of information, particularly about the partitioning of the π-electrons among the rings of the benzenoids and thus their local aromatic properties.

The 'empty ring' concept of Clar's theory is well represented in the MESP maps of triphenylene and dibenzo[*e*,*l*]pyrene. The 'empty ring' is clearly visible in the cases of coronene and perylene (Fig. 4a and c). However, since the outer rings in coronene and perylene are equally liable to possess a sextet, their MESP maps are seen to encompass all the peripheral

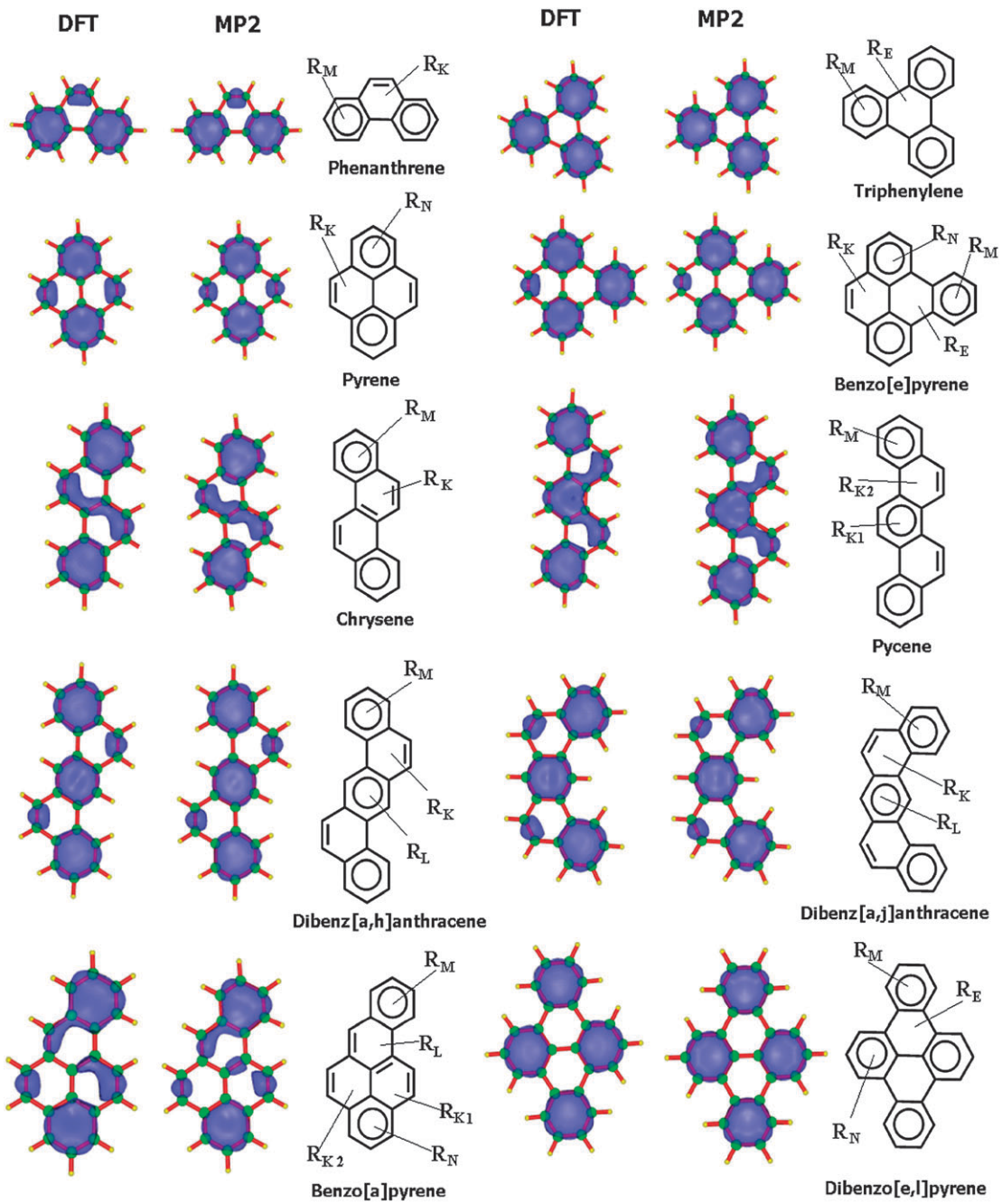

Fig. 3 Illustration of the aromaticity concept based on Clar's theory employing the molecular electrostatic potential maps of selected PAHs at isosurfaces of 11 kcal mol^{-1} at the DFT level and 14 kcal mol^{-1} at the MP2 level. The notations used for characterizing the rings are also shown.

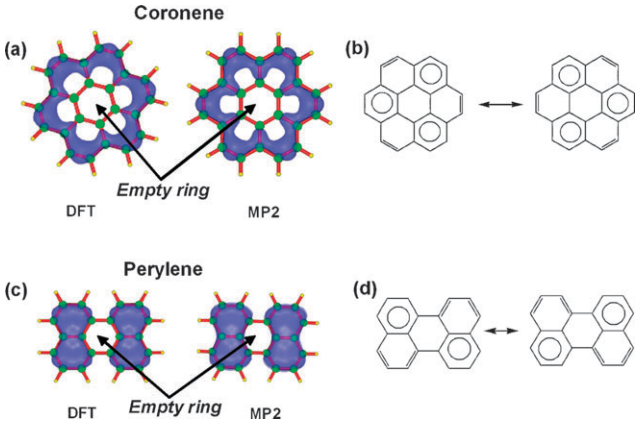

Fig. 4 The empty ring concept of Clar's theory is expressed using MESP isosurfaces at DFT (−11 kcal mol^{-1}) and MP2 (13.5 kcal mol^{-1}) levels for (a) coronene and (b) perylene, and Clar structures for (c) coronene and (d) perylene.

rings equally, leaving the inner ring empty. This feature can be explained by invoking the superposition of the possible resonance structures given in Fig. 4b and d. It may be noted that the symmetric structure of coronene imposes equal bond lengths (1.429 Å at DFT and 1.425 Å at MP2) on all the CC bonds of the empty ring, and they show only a small deviation of 0.029 Å from the typical aromatic CC distance of 1.400 Å. However, the bond length equalization observed herein cannot be used as a criterion to suggest high aromaticity for the inner ring because the MESP map clearly shows that the delocalized electrons are shared primarily in the peripheral rings. In the case of triphenylene, perylene and dibenzo[*e*,*l*]pyrene, the CC bonds of the inner rings that are not shared with the sextet rings (Fig. 3) show considerable deviation from the typical aromatic CC distance (a deviation in the range of 0.049–0.078 Å at DFT and 0.044–0.073 Å at MP2 levels), and this feature supports small values of aromaticity for the central ring. Molecules such as phenanthrene, pyrene, benzo[*e*]pyrene, dibenzo[*a*,*h*]anthracene, dibenzo[*a*,*j*]anthracene are characterized by the presence of localized double bonds separating the aromatic sextets in their Clar structures. This distinguishing feature is reflected very clearly in the MESP map in the form of a localized MESP lobe over the double bond region. In the case of chrysene, the MESP isosurface lobes appear for the end rings, which encompass the corresponding ring carbon atoms and thus represent the main Clar structure given in Fig. 3. Largely a localized distribution of MESP is visible in the middle ring of chrysene, which can be translated into three double bonds, as given in the schematic structure (Fig. 3).

The qualitative agreement of MESP isosurface features with those anticipated from Clar's theory prompted us to look into a more rigorous topographical analysis of MESP of the π-system in every ring. In the MESP topography, the π-region of each ring shows a negatively valued ring CP with a (3, −1) signature. The value of this ring CP is designated as V_{rcp}. The MESP corresponding to V_{rcp} can be used as an electronic descriptor to quantify the relative difference in the π-electron distribution of various type of rings. Analysis of V_{rcp} may also provide insights in to the local aromaticity of individual rings. In Table 1, the V_{rcp} values are given for all the rings at MP2 and DFT levels.

A comparative look at the values computed by the two different theories immediately points out that the MP2 level gives higher negative values of V_{rcp} than the DFT level. Both DFT and MP2 level V_{rcp} values show that the M and N regions are distinctly more electron rich than the K and L regions. However, in the case of linear molecules, at the MP2 level, the L ring values become more negative than the M ring values. Consequently, anthracene and tetracene show L ring V_{rcp} values of −14.38 and −13.61 kcal mol^{-1}, respectively, at the MP2 level that are deeper than the corresponding M values of −14.02 and −13.29 kcal mol^{-1}. The V_{rcp} values at the DFT level for linear systems *viz*. naphthalene, anthracene and tetracene are, respectively, −11.86, −11.04 and −10.72 kcal mol^{-1} for the M rings, and −10.84, −10.51 and −10.04 kcal mol^{-1} for the L rings. The gradually decreasing negative character of the MESP robustly supports Clar's aromatic dilution concept in these linear polyacenes.

In spite of the differences stated above, the MESP values computed by both the theories support Clar's aromatic theory numerically. In general, Clar's sextet-possessing rings, such as M, N and L, are characterized by deeper V_{rcp} values for all the PAH molecules studied. Only in the case of picene, a K ring has a sextet and the V_{rcp} value is −14.47 kcal mol^{-1} (MP2), which is the most negative among all the K rings. At the MP2 level, the most negative V_{rcp} value is calculated for the M ring of triphenylene (−16.04 kcal mol^{-1}), followed by the M ring of phenanthrene (−15.85 kcal mol^{-1}). In all the systems, the least negative values are shown by E rings, the lowest being −11.86 kcal mol^{-1} (MP2) for dibenzo[*e*,*l*]pyrene. This feature is in agreement with the 'empty ring' concept of Clar. The above-described trend of MP2 level V_{rcp} values is followed by the DFT method as well.

Hydrogenation energy and HOMA index

The MESP maps clearly indicate probable regions of sextets and localized double bonds in PAH systems. If hydrogenation (the addition of one H_2) of a ring containing a sextet occurs, it may destroy the aromatic character as this leads to a saturated CC bond. On the other hand, aromatic sextets in the molecule are unaffected if hydrogenation occurs in a region showing localized double bond character (mostly K regions). For instance, in the case of phenanthrene, the hydrogenation of the M ring will destroy one of the sextets, whereas if the addition is on the localized double bond in the K region, both sextets will remain in the resulting molecule.

Hydrogenation of the most aromatic ring is expected to give the least stable product as the stabilizing aromatization energy of that ring will be lost. In the case of benzene, the hydrogenation (at DFT level) is found to be 3.96 kcal mol^{-1} endothermic. On the other hand, the M and K rings of phenanthrene show 4.75 and 15.41 kcal mol^{-1} exothermic characters. The hydrogenation energy (E_H) for the shortest HC–CH bond in the M ring, as well as the HC–CH bond in the K ring, of all the PAH systems are depicted in Table 2. All are exothermic reactions, except for the case of benzene. In fact, benzene is the most aromatic and also the most difficult to

Table 1 The MESP V_{rcp} at the ring CPs of the π-clouds (kcal mol^{-1}) for the PAH systems. See Fig. 2 for the names of the PAHs

		Ring CPs	
PAH	Type of ring	(DFT)	(MP2)
1	R	−14.45	−17.95
2	R_M	−11.86	−15.26
3	(R_M, R_L)	(−11.04, −10.84)	(−14.02, −14.38)
4	(R_M, R_K)	(−12.17, −10.51)	(−15.85, −13.42)
5	(R_M, R_L)	(−10.72, −10.44)	(−13.29, −13.61)
6	(R_{M1}, R_{M2} R_K, R_L)	(−12.11, −11.06, −9.95, −10.96)	(−15.82, −14.14, −12.43, −14.14)
7	(R_M, R_K)	(−11.92, −10.78)	(−15.27, −13.85)
8	(R_M, R_E)	(−12.49, −9.60)	(−16.04, −12.23)
9	(R_N, R_K)	(−11.14, −10.31)	(−14.71, −12.87)
10	(R_M, R_N, R_K, R_E)	(−12.05, −11.42, −10.18, −9.53)	(−15.77, −14.95, −12.83, −12.73)
11	(R_N, R_E)	(−11.22, −9.34)	(−14.49, −11.30)
12	(R_M, R_K, R_L)	(−12.5, −9.92, −11.15)	(−15.50, −12.48, −14.72)
13	(R_M, R_K, R_L)	(−11.86, −11.02, −10.49)	(−15.13, −14.47, −13.46)
14	(R_M, R_K, R_L)	(−11.73, −9.93, −11.18)	(−15.49, −12.52, −14.82)
15	(R_M, R_N, R_{K1}, R_{K2}, R_L)	(−11.36, −10.93, −10.44, −9.87, −10.14)	(−14.74, −14.42, −13.29, −12.13, −13.39)
16	(R_M, R_{K1}, R_{K2}, R_L)	(−11.42, −10.60, −9.60, −9.91)	(−14.79, −13.78, −11.62, −13.00)
17	(R_M, R_N, R_E)	(−12.17, −11.67, −9.53)	(−15.62, −15.16, −11.86)
18	(R_K, R_E)	(−10.01, −9.16)	(−14.49, −13.07)

hydrogenate. A PAH showing the highest exothermicity for a ring is expected to be the lowest in aromatic character. Since, in all hydrogenation products, a saturated CC bond and two new C–H bonds are formed, the relative difference in the hydrogenation energy can be accounted for mainly in the difference in the aromatic character of the systems. Since benzene is the most aromatic, its energy of hydrogenation can be used as a reference to evaluate the aromatization effect of other PAH systems. Most accurate calculations suggest that the aromatic stabilization energy of benzene is close to a value of 30.0 kcal mol^{-1}.[48,49] Hence, the relative value of the hydrogenation energy of all the systems with respect to a reference value of benzene, taken as 30.0 kcal mol^{-1}, can give us a thermodynamic measure of the aromaticity, and this quantity is termed E_{aroma}. The E_{aroma} values are also given in Table 2.

We have also calculated the HOMA index at both DFT and MP2 levels (Table 2) for all the systems using the procedure given by Kruszewski and Krygowski.[15] The E_{aroma} values in Table 2 showed the highest values in the range 18 to 23 kcal mol^{-1} for the M rings in every PAH. Interestingly, all the M rings also showed the highest HOMA index (greater than 0.8), as well as the deepest MESP V_{rcp} values (around −15 kcal mol^{-1} at the MP2 level). Thus, the V_{rcp}, E_{aroma} and HOMA data strongly support Clar's concept of localized π sextets in the peripheral M rings. In the case of linear polyacenes, the E_{aroma} values change drastically when going from benzene to tetracene. For instance, the M rings of naphthalene, anthracene and tetracene showed a decreasing aromatic stability of 18.16, 13.64 and 11.64 kcal mol^{-1}, respectively. A decreasing trend in aromaticity was also observed in their HOMA aromaticity index (naphthalene 0.753, anthracene 0.616 and tetracene 0.520 by DFT), and this trend can also be correlated with their V_{rcp} values. These results support Clar's aromatic dilution concept for linear PAH systems.

A good correlation between E_{aroma} and the HOMA index (the correlation coefficient, R, is 0.965 at the DFT level and 0.963 at the MP2 level) is obtained that supports the use of E_{aroma} as a good measure of the energy component of local aromatization in PAHs. The MESP V_{rcp} values calculated at both the DFT and MP2 levels also show good correlations with E_{aroma} (Fig. 5). In these correlations, coronene is considered an exception because the peripheral rings of this molecule are not fully developed into a sextet and therefore the hydrogenation energy may not fully account for the destabilization due to the removal of a sextet. The correlation equations presented in Fig. 5 can be used for predicting the E_{aroma} value of any ring if V_{rcp} is known. Thus, according to the DFT level correlation, the empty ring of coronene, perylene, benzo[*e*,*l*]pyrene and triphenylene have smaller E_{aroma} values of 5.74, 6.65, 7.62 and 7.97 kcal mol^{-1}, respectively, when compared to other rings. Similarly, moderately high values of E_{aroma} (14.72 to 18.47 kcal mol^{-1}) are observed for the N rings of all the systems. The E_{aroma} value of the L rings is in the range 9.54 to 15.98 kcal mol^{-1}.

Recently, Palusiak and Krygowski[50] have analyzed the 'atoms in molecule' parameters at the ring CPs of five PAH systems (benzene, naphthalene, anthracene, phenanthrene and triphenylene) at the MP2/6-31G(2d,p) level and observed a good linear relationship between the density of the total electron energy, H, at the CPs and the HOMA index. They recommended the use of H as an electron density-based quantitative characteristic of π-electron delocalization. A comparison of H and V_{rcp} at the MP2 level showed that a more positive H corresponds to a more negative V_{rcp}, suggesting the electron rich character of the ring. The H values of the M rings of all the molecules showed a near perfect correlation (R = 0.994) with V_{rcp}, while the inclusion of inner rings in the correlation decreased the R value to 0.914. It is worth noting that the E_{aroma} and H values also showed a strong correlation (R = 0.994). The H values (in kcal mol^{-1} bohr^{-1} units) taken from ref. 50 are 5.128 for benzene, 5.000 for naphthalene, 4.953 (outer ring) and 4.905 (inner ring) for anthracene, 5.032 (outer ring) and 4.813 (inner ring) for phenanthrene, and 5.054 (outer ring) and 4.557 (inner ring) for triphenylene.

Table 2 MESP V_{rcp} values (kcal mol^{-1}) of M and K type rings. The E_H (kcal mol^{-1}), E_{aroma} (kcal mol^{-1}) and HOMA index values are also depicted

	V_{rcp} for M and K rings				HOMA	
Molecule	(DFT)	(MP2)	E_H (DFT)	E_{aroma} (DFT)	(DFT)	(MP2)
Benzene	−14.45	−17.95	3.96	30.00	1.000	1.000
Naphthalene	M −11.86	−15.26	−7.88	18.16	0.753	0.869
Anthracene	M −11.04	−14.02	−12.40	13.64	0.616	0.772
Phenanthrene	M −12.17	−15.85	−4.75	21.29	0.857	0.919
	K −10.51	−13.42	−15.41	10.63	0.433	0.659
Tetracene	M −10.72	−13.29	−14.40	11.64	0.520	0.734
Benz[*a*]anthracene	M1 −12.11	−15.82	−3.35	22.69	0.873	0.939
	M2 −11.06	−14.14	−10.71	15.33	0.683	0.818
	K −9.95	−12.43	−17.87	8.17	0.247	0.549
Chrysene	M −11.92	−15.27	−5.92	20.12	0.828	0.908
	K −10.78	−13.85	−13.92	12.12	0.542	0.727
Triphenylene	M −12.49	−16.04	−3.67	22.37	0.877	0.942
Pyrene	K −10.31	−12.87	−14.52	11.52	0.537	0.745
Benzo[*e*]pyrene	M −12.05	−15.77	−3.62	22.42	0.838	0.940
	K −10.18	−12.83	−14.26	11.78	0.521	0.716
Dibenz[*a*,*h*]anthracene	M −12.5	−15.5	−3.92	22.12	0.864	0.933
	K −9.92	−12.48	−16.94	9.10	0.329	0.606
Picene	M −11.86	−15.13	−5.63	20.41	0.834	0.914
	K1 −10.49	−13.46	−14.51	11.53	0.505	0.713
	K2 −11.02	−14.47	−11.89	14.15	0.627	0.789
Dibenz[*a*,*j*]anthracene	M −11.73	−15.49	−3.98	22.06	0.864	0.930
	K −9.93	−12.52	−17.11	8.93	0.327	0.599
Benzo[*a*]pyrene	M −11.36	−14.74	−8.03	18.01	0.771	0.860
	K1 −10.44	−13.29	−12.40	13.64	0.646	0.797
	K2 −9.87	−12.13	−16.70	9.34	0.429	0.679
Dibenzo[*a*,*i*]pyrene	M −11.42	−15.62	−6.80	19.24	0.809	0.879
	K2 −9.60	−11.62	−17.96	8.08	0.320	0.614
Dibenzo[*e*,*l*]pyrene	M −12.47	−15.49	−3.97	22.07	0.885	0.948
Coronene	K −10.01	−13.49	−9.03	17.01	0.696	0.846

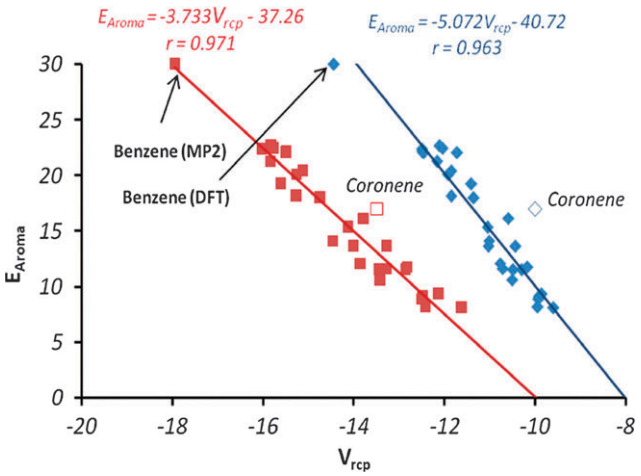

Fig. 5 The correlation between V_{rcp} and relative hydrogenation energy (E_{aroma}) values. Both MP2 and DFT level V_{rcp} values are correlated. All values are given in kcal mol^{-1}.

Conclusion

A strong correlation between Clar's aromatic sextet theory and MESP topographical features of the π-regions of PAH molecules were obtained in this work. MESP maps provided useful pictorial representations of Clar's theory. Furthermore, negatively valued ring CPs (V_{rcp}) of the MESP located for the π-regions of each aromatic ring were found to be a good local measure of aromaticity. The V_{rcp} values correlated well with the thermodynamic measure of aromaticity, E_{aroma}. A good correlation was also obtained between V_{rcp} and the geometric index of aromaticity, HOMA. In summary, we have demonstrated that MESP maps and the corresponding V_{rcp} values are simple and efficient probes to represent Clar's aromatic features of a PAH system. We also wish to note that the main aim of this study is to demonstrate the intimate relationship between Clar's theory and MESP, and not to propose another new index of aromaticity.

Acknowledgements

Support of this work by the Department of Science and Technology, India, grant number SR/FTP/CS-116/2005, is gratefully acknowledged.

References

1 M. Randić, *Chem. Rev.*, 2003, **103**, 3449.
2 E. Hückel, *Z. Phys.*, 1931, **70**, 204.
3 V. J. Minkin, M. N. Glukhovtsev and B. Y. Simkin, *Aromaticity and Antiaromaticity: Electronic and Structural Aspects*, Wiley, New York, 1994.
4 E. Clar, *Polycyclic Hydrocarbons*, Academic Press, London, 1964.
5 E. Clar, *The Aromatic Sextet*, Wiley, London, 1972.
6 I. Gutman and S. J. Cyvin, *Introduction to the Theory of Benzenoid Hydrocarbons*, Springer, Berlin, 1989.
7 M. D. Watson, A. Fechtenkötter and K. Müllen, *Chem. Rev.*, 2001, **101**, 1267.
8 I. Gutman, Z. Tomović, K. Müllen and J. P. Rabe, *Chem. Phys. Lett.*, 2004, **397**, 412.

9 O. E. Polansky and G. Derflinger, *Int. J. Quantum Chem.*, 1967, **1**, 379.
10 H. Zhu and Y. Jiang, *Chem. Phys. Lett.*, 1992, **193**, 446.
11 Z. B. Maksić, D. Barić and T. J. Müller, *J. Phys. Chem. A*, 2006, **110**, 10135.
12 J.-I. Aihara, T. Ishida and H. Kanno, *Bull. Chem. Soc. Jpn.*, 2007, **80**, 1518.
13 G. Portella, J. Poater and M. Solà, *J. Phys. Org. Chem.*, 2005, **18**, 785.
14 A. Misra, D. J. Klein and T. J. Morikawa, *J. Phys. Chem. A*, 2009, **113**, 1151.
15 J. Kruszewski and T. M. Krygowski, *Tetrahedron Lett.*, 1972, **13**, 3839.
16 T. M. Krygowski, *J. Chem. Inf. Comput. Sci.*, 1993, **33**, 70.
17 F. Feixas, E. Matito, J. Poater and M. J. Solà, *J. Comput. Chem.*, 2008, **29**, 1543.
18 P. v. R. Schleyer, C. Maerker, A. Dransfeld, H. Jiao and N. J. v. E. Hommes, *J. Am. Chem. Soc.*, 1996, **118**, 6317.
19 P. v. R. Schleyer, H. Jiao, N. J. v. E. Hommes, V. G. Malkin and O. Malkina, *J. Am. Chem. Soc.*, 1997, **119**, 12669.
20 M. K. Cyrañski, T. M. Krygowski, A. R. Katritzky and P. v. R. Schleyer, *J. Org. Chem.*, 2002, **67**, 1333.
21 A. Lazzeretti, *Phys. Chem. Chem. Phys.*, 2004, **6**, 217.
22 R. W. A. Havenith and P. W. Fowler, *Phys. Chem. Chem. Phys.*, 2006, **8**, 3383.
23 Y.-C. Lin, J. Jusélius, D. Sundholm and J. Gauss, *J. Chem. Phys.*, 2005, **122**, 214308.
24 P. Lazzeretti, M. Malagoli and R. Zanasi, *Chem. Phys. Lett.*, 1994, **220**, 299.
25 R. Zanasi, P. Lazzeretti, M. Malagoli and F. Piccinini, *J. Chem. Phys.*, 1995, **102**, 7150.
26 T. A. Keith and R. F. W. Bader, *Chem. Phys. Lett.*, 1993, **210**, 223.
27 M. A. Spackman and R. F. Stewart, in *Chemical Applications of Atomic and Molecular Electrostatic Potentials*, ed. P. Politzer and D. G. Truhlar, Plenum, New York, 1981, p. 407.
28 P. Bultinck, M. Rafat, R. Ponec, B. v. Gheluwe, R. Carbo-Dorca and P. Popelier, *J. Phys. Chem. A*, 2006, **110**, 7642.
29 J. Poater, X. Fradera, M. Duran and M. Solà, *Chem.–Eur. J.*, 2003, **9**, 1113.
30 R. F. W. Bader, *Atoms in Molecules, a Quantum Theory*, Clarendon Press, Oxford, 1990.
31 E. Scrocco and J. Tomasi, *Adv. Quantum Chem.*, 1978, **11**, 116.
32 P. Politzer and D. G. Truhlar, *Chemical Applications of Atomic and Molecular Electrostatic Potentials*, Plenum, New York, 1981.
33 T. Brinck, J. S. Murray and P. Politzer, *Int. J. Quantum Chem.*, 1993, **48**, 73.
34 P. Politzer, J. S. Murray and M. C. Concha, *Int. J. Quantum Chem.*, 2002, **88**, 19.
35 P. Politzer and J. S. Murray, *Theor. Chem. Acta*, 2002, **108**, 134.
36 C. H. Suresh and S. R. Gadre, *J. Org. Chem.*, 1999, **64**, 2505.
37 S. R. Gadre and S. S. Pundlik, *J. Am. Chem. Soc.*, 1995, **117**, 9559.
38 C. H. Suresh and S. R. Gadre, *J. Phys. Chem. A*, 2007, **111**, 710.
39 C. H. Suresh, N. Koga and S. R. Gadre, *Organometallics*, 2000, **19**, 3008.
40 C. H. Suresh, N. Koga and S. R. Gadre, *J. Org. Chem.*, 2001, **66**, 6883.
41 R. G. Harvey, *Polycyclic Aromatic Hydrocarbons: Chemistry and Carcinogenicity*, Cambridge University Press, Cambridge, 1991, pp. 1–4.
42 K. P. Vijayalakshmi and C. H. Suresh, *J. Comput. Chem.*, 2008, **29**, 1808.
43 K. P. Vijayalakshmi and C. H. Suresh, *Org. Biomol. Chem.*, 2008, **6**, 4384.
44 M. J. Frisch, G. W. Trucks, H. B. Schlegel, G. E. Scuseria, M. A. Robb, J. R. Cheeseman, J. A. Montgomery, Jr., T. Vreven, K. N. Kudin, J. C. Burant, J. M. Millam, S. S. Iyengar, J. Tomasi, V. Barone, B. Mennucci, M. Cossi, G. Scalmani, N. Rega, G. A. Petersson, H. Nakatsuji, M. Hada, M. Ehara, K. Toyota, R. Fukuda, J. Hasegawa, M. Ishida, T. Nakajima, Y. Honda, O. Kitao, H. Nakai, M. Klene, X. Li, J. E. Knox, H. P. Hratchian, J. B. Cross, V. Bakken, C. Adamo, J. Jaramillo, R. Gomperts, R. E. Stratmann, O. Yazyev, A. J. Austin, R. Cammi, C. Pomelli, J. Ochterski, P. Y. Ayala, K. Morokuma, G. A. Voth, P. Salvador, J. J. Dannenberg, V. G. Zakrzewski, S. Dapprich, A. D. Daniels, M. C. Strain, O. Farkas, D. K. Malick, A. D. Rabuck, K. Raghavachari, J. B. Foresman, J. V. Ortiz, Q. Cui, A. G. Baboul, S. Clifford, J. Cioslowski, B. B. Stefanov, G. Liu, A. Liashenko, P. Piskorz, I. Komaromi, R. L. Martin, D. J. Fox, T. Keith, M. A. Al-Laham, C. Y. Peng, A. Nanayakkara, M. Challacombe, P. M. W. Gill, B. G. Johnson, W. Chen, M. W. Wong, C. Gonzalez and J. A. Pople, *GAUSSIAN 03 (Revision C.02)*, Gaussian, Inc., Wallingford, CT, 2004.
45 S. R. Gadre and R. N. Shirsat, *Electrostatics of Atoms and Molecules*, Universities Press, Hyderabad, India, 2000.
46 R. N. Shirsat, S. V. Bapat and S. R. Gadre, *Chem. Phys. Lett.*, 1992, **200**, 373.
47 A. C. Limaye and S. R. Gadre, *Curr. Sci.*, 2001, **80**, 1296.
48 P. v. R. Schleyer and F. Puhlhofer, *Org. Lett.*, 2002, **4**, 2873.
49 C. H. Suresh and N. Koga, *J. Org. Chem.*, 2002, **67**, 1965.
50 M. Palusiak and T. M. Krygowski, *Chem.–Eur. J.*, 2007, **13**, 7996.

